Cell, Volume *139*

Supplemental Data

Retinal Input Instructs Alignment of Visual Topographic Maps

Jason W. Triplett, Melinda T. Owens, Jena Yamada, Greg Lemke, Jianhua Cang, Michael P. Stryker, and David A. Feldheim

SUPPLEMENTAL EXPERIMENTAL PROCEDURES

Receptor affinity probe *in situ*

EphA3-AP and ephrin-A5-AP *in situ* staining was done essentially as described (Feldheim et al., 1998), with some modifications. Postnatal day 8 brains were dissected and fixed 15 min in 4% paraformaldehyde at 4°C. After washing in PBS, brains were embedded in 5% agarose in PBS on ice. Parasagittal sections were cut 250 μm thick with a manual Vibroslice (World Precision Instruments, Sarasota) and collected in ice-cold PBS. Sections containing the SC were treated with either AP, EphA3-AP or ephrin-A5 AP (Cheng et al., 1995), washed in Hepes buffered saline (HBS, 20 mM Hepes pH 7.0), post-fixed in 40% acetone/10% formalin pH 6.2 for 1 min, washed in HBS, and heat-inactivated in HBS at 65°C overnight. The following morning, sections were washed in HBS and AP reaction was carried out at room temperature.

SUPPLEMENTAL FIGURE LEGENDS

Figure S1. Comparison of anterior and posterior SC functional maps in EphA3$^{ki/ki}$ mice

(A) Quantification of the area of anterior and posterior SC functional maps in EphA3$^{ki/ki}$ mice. Data are represented as mean +/- SEM. N = 9.

(B) Quantification of signal strength from anterior and posterior maps in EphA3$^{ki/ki}$ mice. Data are represented as mean +/- SEM. *, P = 0.007, two-tailed student's t-test; N = 9.

(C) Distribution of anterior to posterior amplitude ratios in EphA3$^{ki/ki}$ mice. *bars*, mean +/- SEM; N = 9.

Figure S2. The retinogeniculate and geniculocortical projections are not anatomically duplicated in EphA3$^{ki/ki}$ mice

(A) Whole mount view of the SC after focal injection of DiI in nasal retina. In EphA3$^{ki/ki}$ mice, two TZs (arrowheads) were observed in the central and posterior SC. *dashed area*, SC; *inset*, schematic of retinal injection site; N, nasal; T, temporal; M, medial; P, posterior. N = 8.

(B) Coronal section through the LGN after focal injection of DiI in nasal retina. In EphA3$^{ki/ki}$ mice, a single TZ (arrowhead) was observed in ventral dLGN. *dashed area*, dLGN; D, dorsal; M, medial. N = 8. Images in (A) and (B) are from the same animal.

(C) Image of the cortical surface of V1 (dashed area) prior to intrinsic optical imaging. After imaging, fluorescently tagged CTBs were injected at the indicated locations (green and red dots). A, anterior; L, lateral.

(D) Coronal section through the LGN after focal injection of CTB-594 (red) and CTB-488 (green) in V1. In EphA3$^{ki/ki}$ a single injection in V1 labels dLGN cell somas in a single area. D, dorsal; M, medial. N = 5. Images in (C) and (D) are from the same animal.

Figure S3. Laminar targeting and refinement errors of corticocollicular projections in β2$^{-/-}$ mice

(A) Parasagittal SC section after focal injection of DiI (red) in central V1 and whole eye fill with CTB-488 (green) in the contralateral eye, which labels all RGCs. In WT mice a

single injection gives a single TZ in the central SC. *insert*, schematic of V1 injection site; A, anterior; D, dorsal; *, pretectal nucleus.

(B) Parasagittal SC section after focal injection of DiI (red) in central V1 and whole eye fill with CTb-488 (green) in the contralateral eye, which labels all RGCs. In $\beta2^{-/-}$ mice a single injection gives a single broad TZ in the central SC. *insert*, schematic of V1 injection site; *, pretectal nucleus.

(C) Corticocollicular TZ location expressed as a percent of SC anterior-posterior axis was plotted as a function of V1 injection site expressed as percent of the L-M axis of the cortical hemisphere. Line represents best-fit regression, $R^2 = 0.9118$.

(D) Quantification of TZ area, as a percent of the SC in WT and $\beta2^{-/-}$. Data are represented as mean +/- SEM, N > 7. ***, P < 0.001 vs. WT, Kolmogorov-Smirnov test.

(E) Quantification of TZ overlap with the SC retinal input layer as a percent of TZ area in WT and $\beta2^{-/-}$ mice. Data are represented as mean +/- SEM. *, P < 0.05 vs. WT, Kolmogorov-Smirnov test.

Figure S4. EphA and ephrin-A expression gradients are not altered in the SC of EphA3$^{ki/ki}$ mice

(A & B) Parasagittal SC sections of P8 brains after staining with EphA3-alkaline phosphatase (AP) fusion protein. In WT (A) and EphA3$^{ki/ki}$ (B) mice, there was a high posterior to low anterior gradient of ephrin-A expression. LGN, lateral geniculate nucleus; pt, pretectum; SC, superior colliculus; IC, inferior colliculus; A, anterior; D, dorsal.

(C & D) Parasagittal SC sections after staining with ephrin-A5-AP fusion protein. In WT (C) and EphA3$^{ki/ki}$ (D) mice, there was a high anterior to low posterior gradient of EphA expression.

(E) Parasagittal section after AP only staining. In EphA3$^{ki/ki}$ mice, no significant background staining was observed.

SUPPLEMENTAL REFERENCES

Cheng, H. J., Nakamoto, M., Bergemann, A. D., and Flanagan, J. G. (1995). Complementary gradients in expression and binding of ELF-1 and Mek4 in development of the topographic retinotectal projection map. Cell *82*, 371-381.

Feldheim, D. A., Vanderhaeghen, P., Hansen, M. J., Frisén, J., Lu, Q., Barbacid, M., and Flanagan, J. G. (1998). Topographic guidance labels in a sensory projection to the forebrain. Neuron *21*, 1303-1313.

Supplemental Figure 1

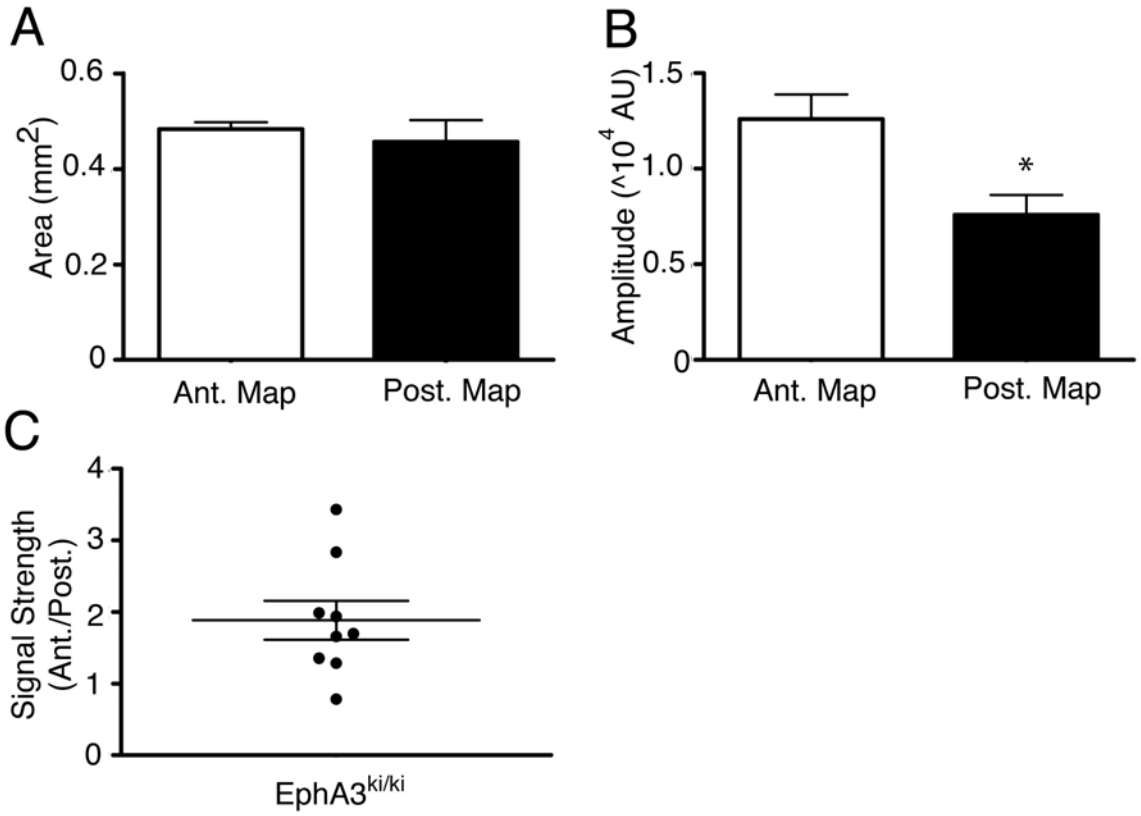

Supplemental Figure 2

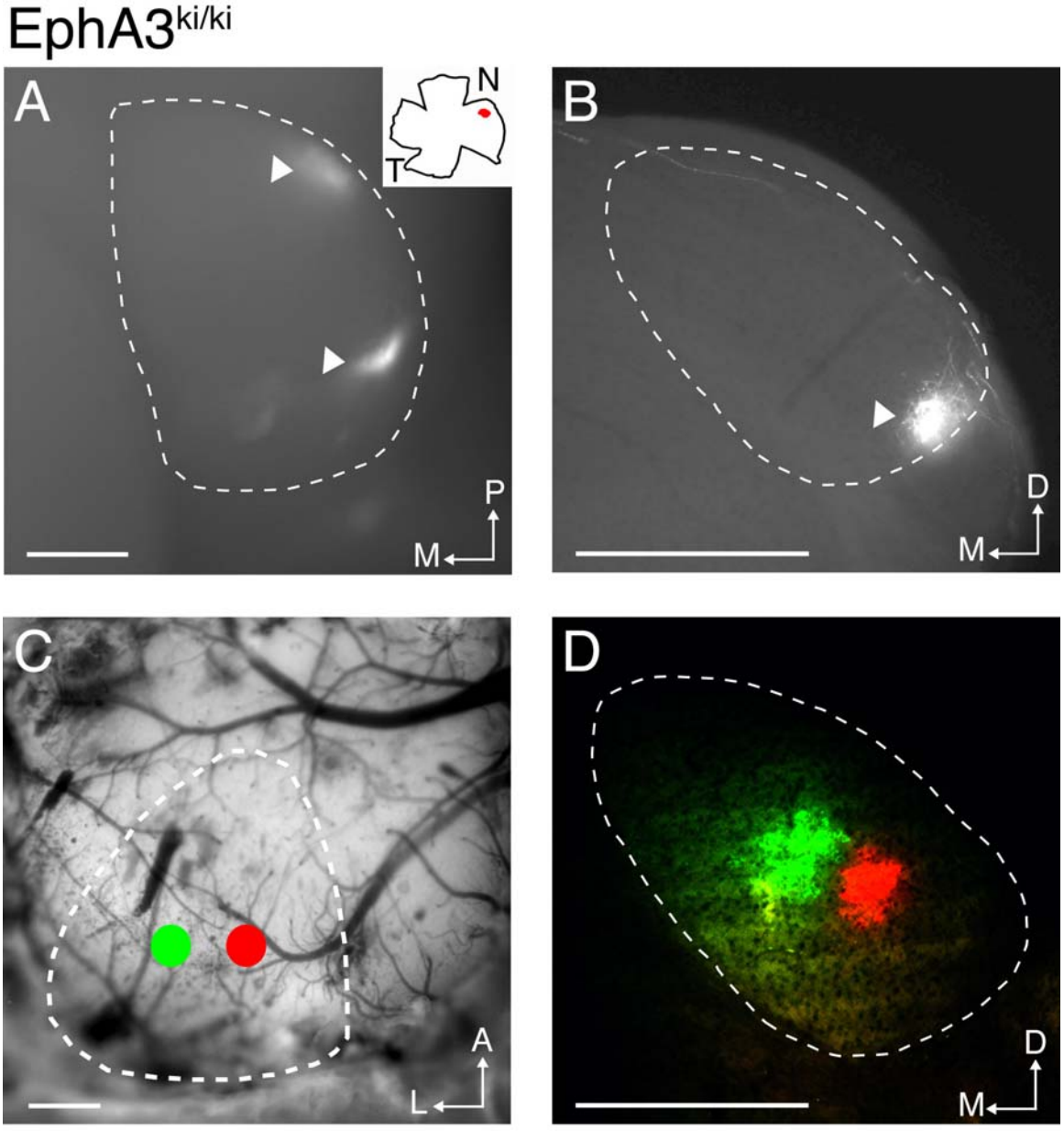

Supplemental Figure 3

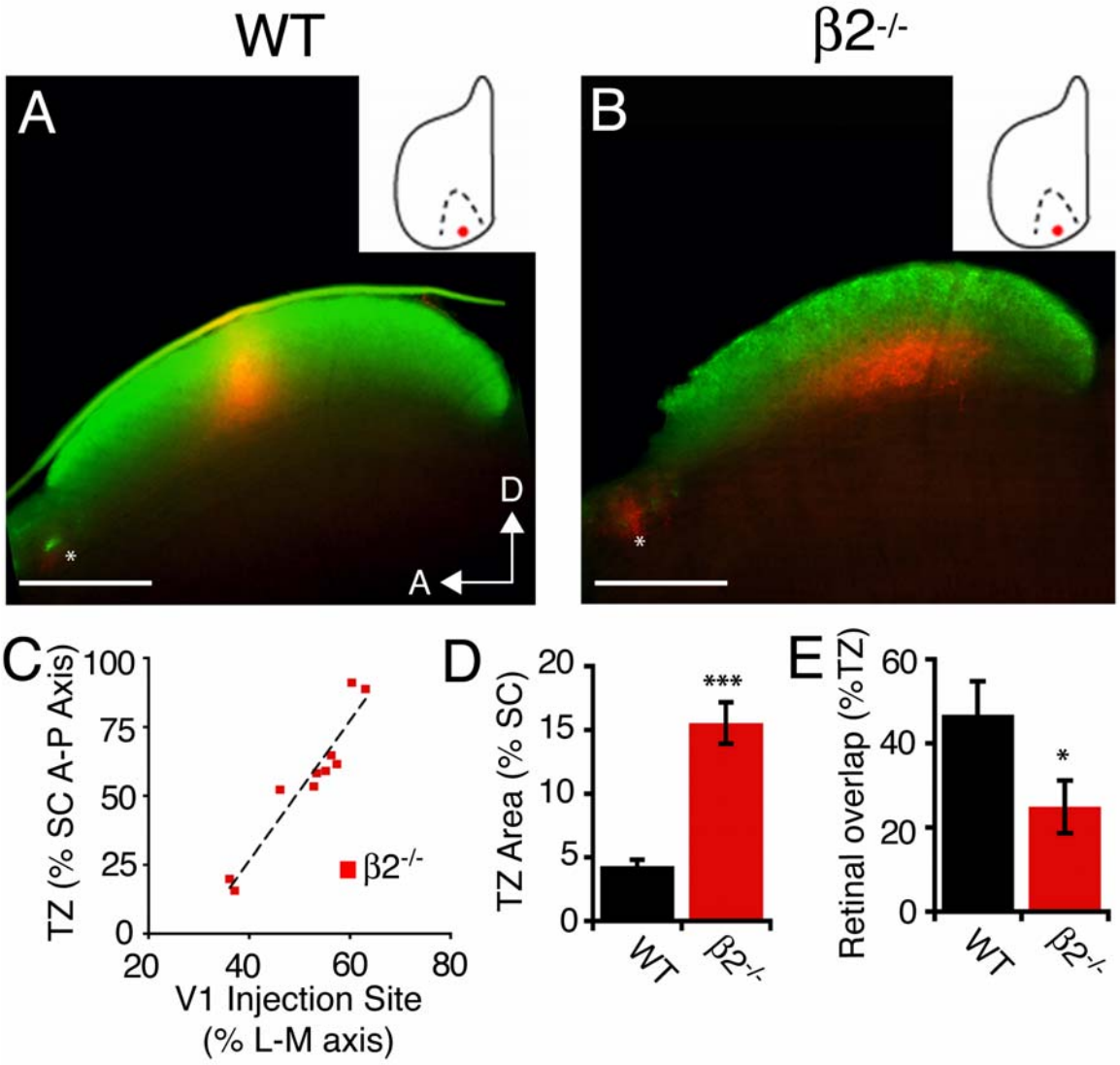

Supplemental Figure 4